Chaos, Solitons and Fractals 160 (2022) 112171

Contents lists available at ScienceDirect

Chaos, Solitons and Fractals

Nonlinear Science, and Nonequilibrium and Complex Phenomena

journal homepage: www.elsevier.com/locate/chaos

Complex regimes in electronic neuron-like oscillators with sigmoid coupling

Nikita M. Egorov [a], Ilya V. Sysoev [b,*], Vladimir I. Ponomarenko [c], Marina V. Sysoeva [a]

[a] Yuri Gagarin State Technical University of Saratov, 77 Politechnicheskaya, Saratov, Russia
[b] Saratov State University, 83, Astrakhanskaya str., Saratov, Russia
[c] Saratov Branch of Institute of Radioengineering and Electronics of RAS, 38, Zelenaya str., Saratov, Russia

ARTICLE INFO

Article history:
Received 24 March 2022
Received in revised form 26 April 2022
Accepted 27 April 2022
Available online xxxx

Keywords:
FitzHugh–Nagumo neuron
Electronic oscillator
Sigmoid coupling
Coupled generators
Transient process

ABSTRACT

The new version of electronic implementation of FitzHugh–Nagumo neuron model was proposed together with a new circuit for synapse (sigmoid activation function). The proposed neuron and synapse models provide better representation of activation function in biological neurons including possibility to model excitatory and inhibitory connections. Various regimes in two FitzHugh–Nagumo neurons were studied numerically and in hardware experiment. Different scenarios of oscillation emergence were investigated, including saddle-node cycle bifurcation leading to appearance of highly nonlinear limit cycles of large amplitude. Long living transients near these bifurcations were found those are of particular interest for modeling some metastable phenomena in living systems like sleep and epilepsy.

1. Introduction

Interest to the brain dynamics led to construction of electronic (silicon) neurons. The first realization [1] tried to implement Hodgkin–Huxley neuron [2] since this mathematical model was considered as a reference at the time. The next realizations [3,4] improved this circuit. Then, realizations of other mathematical neuron models appeared, including FitzHugh-Nagumo [5,6] neuron electronic realizations [7–9]. A wish to be able to model large numbers of neurons which can adequately represent dynamics of real brain led to miniaturization and construction of arrays of electronic neurons with synapses [10], which can work in real time including hybrid analog-digital systems [11]. The problem of such an approach is that the individual properties of such neurons are hardly to be controlled and the gap between results obtained in mathematical models and obtained in hardware becomes too large (actually, often there is no direct correspondence between them). Therefore, the large scale neuron models have been still developed [9].

Electronic circuit models have the large advantage over mathematical models in application to live nature phenomena, since they represent three main properties of biological systems. First, electronic circuits are not completely stationary due to characteristics of their components depend on temperature, humidity and other conditions. This makes the results obtained from electronic circuits more robust, since the fragile regimes are not realized. Therefore, regimes realized in electronic models are more likely to be found in the underlying biological object. Second, the components of electronic circuits are not completely equal, and therefore unrealistic degenerate regimes cannot appear in these models. Third, the measurement procedure for electronic circuit is much closer to the biological one than for the mathematical model. All these points make the electronic circuits to be a good and promising step in modeling biological phenomena.

Recently, electronic circuits constructed from traditional elements occurred to be efficient for modeling some types of brain activity even though the number of neurons was not large. In particular, in [12,13] the radioengineering realization of mesoscale hierarchically organized neural network model of brain thalamocortical system was proposed. This network was proven to generate epileptiform activity in response to external input in the form of a short sequence of pulses [14], which is a valid scenario of seizure initiation as shown for both humans and rats [15]. In this scenario an external input from peripheral nervous system (e. g. from nervus trigeminus) excites the thalamus and provokes a seizure.

The model [12] together with its mathematical origin [16] consists of 14 model cells and it is a result of downscaling of the larger model [17] consisting of 500 neurons, when the desired regimes are kept. Since the connectivity matrix of the model has to be anatomically relevant and arbitrary couplings are not possible, the minimal number of neurons

* Corresponding author.
E-mail address: ivssci@gmail.com (I.V. Sysoev).

https://doi.org/10.1016/j.chaos.2022.112171
0960-0779/

cannot be very small. In particular, for 14-element matrices the quantitative representation of experimental phenomena, which was accurate for 500-element models, occurred to be not possible and only qualitative match was achieved. If the number of model electronic neurons increases the experimentally observed dynamics is represented better [14], but this demands much larger engineering. However, at the same point, even the 14-element models occurred to be too complex for analytical and even numerical study. The former simplified models like proposed in [7,9] also have two main disadvantages. First, for simplicity, the reduced FitzHugh–Nagumo model proposed in [18] was used in [12] to reduce the number of parameters and since this model was already realized as a device [9]. This simplified model does not allow to separate excitatory and inhibitory connectivity, since if parameter b=0, the mean value of external driving can be set zero by renormalization of variables and the parameter a in the model, see Eq. (1) for details. Second, the connectivity was linear, but such an approach is not very accurate. If activation is modeled as a function without separate systems of equations for a synapse, a sigmoid function is usually used to represent synaptic coupling [19,20]. Actually, in the reduced model all couplings are both excitatory and inhibitory in different phases of oscillation, making synaptic-like connectivity useless (there is no possibility to set the sigmoid always positive or always negative), so it is not possible to solve the second problem until the first still takes place. Two these disadvantages together significantly reduce the relevance of synaptic mechanism description in the model. The current study aims to fix these two disadvantages, providing both new electrical neuron and synapse models together.

To understand the new neuron and synapse models better we focused on a simpler system of two neurons, which can be coupled in different ways, including unidirectional and bidirectional, excitatory and inhibitory couplings. First, we investigated circuit mathematical models to get a fast overview of possible regimes, and then we constructed and studied hardware circuits. The regimes of high amplitude oscillations close in parameter space to the nonoscillatory excitable regimes, when transition takes place due to some nonlocal bifurcation like saddle-node bifurcation of limit cycle [21,22], were of particular interest. These regimes can be candidates for long transients, so they are interesting for modeling some brain regimes [17,23–26].

2. Mathematical model

Each individual neuron was built as complete FitzHugh–Nagumo model [5,6]. All couplings were sigmoid:

$$\begin{aligned} \varepsilon\dot{u}_i(t) &= u_i(t) - c_i u_i^3(t) - v_i(t) + \textstyle\sum_{j\neq i} k_{ij} h(u_j(t)), \\ \dot{v}_i &= u_i(t) + a_i - b_i v_i(t), \end{aligned} \tag{1}$$

$$h(u) = \frac{1 + \tanh(u)}{2}, \tag{2}$$

where u is dimensionless function analogous to the transmembrane potential in biological excitable tissue; v is dimensionless function similar to slow recovery current; t is dimensionless time; ε is inertia parameter; a and b are dimensionless parameters that control the neuron's own dynamics; c is integration constant. The model describes regenerative self-excitation of voltage on the cell membrane (variable u) as a result of nonlinear positive feedback, as well as "recovery" as a result of linear negative current feedback (variable v).

Synapses are described by the activation function. Often, the sigmoid function is used as an activation function in neural networks. The sigmoid activation function means depolarisation within a neuronal population to expected firing rate. It can be interpreted as a cumulative density function on depolarization within a population [20]. Hyperbolic tangent function is classically used as a sigmoid function being a particular case of the more general Richard's curve [27]; in our case it was shifted and scaled to match the desired range [0,1], as it is shown in the formula (2).

In cell biophysics all synapses are divided into excitatory and inhibitory ones. Excitatory (mostly, glutamatergic) synapses facilitate pulse appearance on the postsynaptic membrane, depolarizing it and making the action potential to be possible. In contrary, inhibitory (mostly, GABAergic) synapses prevent or stop generation of action potentials at postsynaptic membrane. In the model (1) the positive values of coupling coefficient k_{ij} correspond to excitatory synapses and negative ones — to inhibitory ones.

3. Electronic realization of a single neuron

A circuit diagram of the constructed complete FitzHugh–Nagumo electronic oscillator is shown in Fig. 1. The circuit contains two analog multipliers U1 and U2 and two dual operational amplifiers U3 and U4. Elements U4B and U3A are integrators, element U4A is a inverter, element U3B is a follower. R_a and R_b are potentiometers that allow you to change the value of parameters a and b. This circuit was constructed in the development of previously constructed reduced electronic oscillator [9], the another scheme different in detail was also proposed previously [7].

In contrast to the mathematical model, see Eq. (1), the parameters of the radioengineering circuit have dimensions. The time-scale parameters have the values $E = R11C1$ and $T = R7C2$. Parameter ε from Eq. (1) is calculated as $\varepsilon = E/T$. Parameters $c = (R3 + R4)/R3$ and $b = R6/\left(R5 + R_b \cdot \frac{B}{100\%}\right)$ (B — percentage of potentiometer R_b used) are scaling factors at U and V respectively. Coupling coefficient k is calculated as $k = R13/R14$.

The parameter a is set by the voltage at the "+" clamp of the amplifier U3B. The total voltage drop on a series-connected resistor $R10 = 5$ kΩ and potentiometer $R_a = 1$ kΩ is $U_a = 15$ V, i. e. the voltage drop on the entire potentiometer is 2.5 V. In particular, if the potentiometer is set to $A = 0\%$, the voltage 2.5 V is set to "+" input of U3B, and if the potentiometer is set to $A = 100\%$, this voltage is zero. So, the parameter a can be calculated using A measured in percents of potentiometer use as follows: $a = 2.5 \cdot \left(1 - \frac{A}{100\%}\right)$. It is set in volts as variables u and v actually do in the scheme (let their dimensional values be denoted as U and V).

The cubic transformation is provided by the amplifiers U1 and U2. Integrators U4B and U3A allow to obtain U and V, respectively. Inverter U4A allows to obtain $-U$. Follower U3B is used for connection to the circuit of potentiometer $R10$. Input $I1$ receive signal from the other neuron.

4. Electronic realization of a synapse

A circuit diagram of the sigmoid activation function is shown in Fig. 2. The scheme was taken from the work [28] with minor changes. The circuit contains a dual operational amplifier U1 and two bipolar junction transistors Q1 and Q2. The inverting amplifier U1A has a gain of 0.05. The differential amplifier U1B has a gain of 0.5. Difference between excitatory and inhibitory couplings was realized by a switcher, which rearranged chip legs 5 and 6 of the amplifier U1B.

Excitatory coupling was organized as $k \cdot h(u)$, k>0. For positive values of u, if the pulse was generated in the driving neuron, the potential at the driven one was increased up to value equal to k, since $0 \le h(u) \le 1$. This could lead to generation of pulse (action potential) at the driven neuron if its one potential plus the driving potential were larger than 0, then, this pulse can spear further along the network. If u<0 for k>0, no significant changes in the dynamics of the driven generator would be caused, since the driving would be zero or close to zero for $u \approx 0$. If $u \approx 0$ some subthreshold oscillations can appear in the driven neuron, but they do not have any significant biological meaning and cannot spread further.

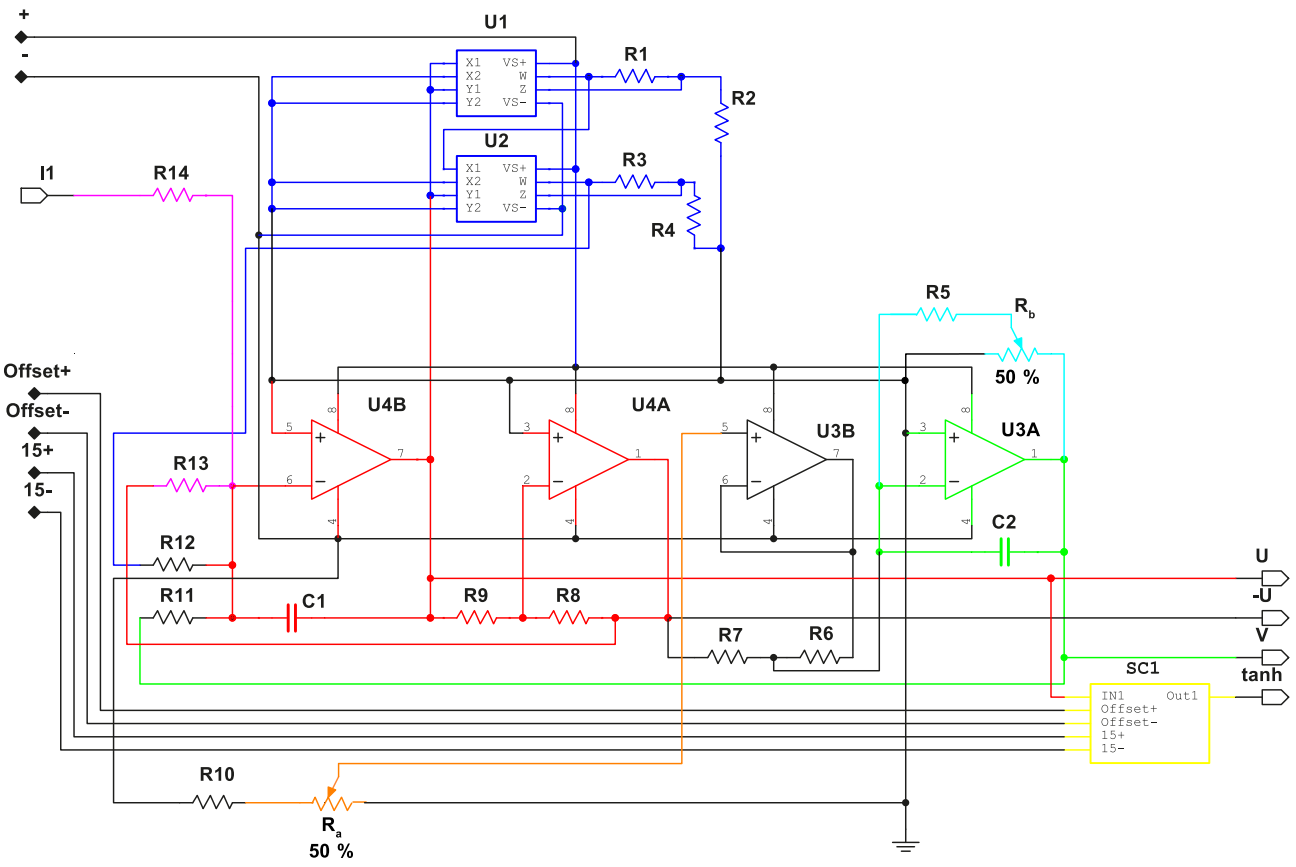

Fig. 1. Circuit diagram of a single complete FitzHugh-Nagumo neuron. Red color: u, blue color: cu^3, green color: $-v$, cyan color: b, orange color: a, pink color: k. $R1 = R3 = 1$ kΩ, $R2 = 9$ kΩ, $R4 = 2.333$ kΩ, $R_a = 1$ kΩ, $R10 = 5$ kΩ, $R_b = 4.7$ MΩ, $R5 = 51$ kΩ, $R6 = R7 = R8 = R9 = R11 = R12 = R13 = 100$ kΩ, $R14$ depends on coupling strength k, $C1 = 1$ nF, $C2 = 0.01$ uF, U1, U2 are analog multipliers of the type AD633, and U3, U4 are operation amplifiers of the type AD822. (For interpretation of the references to color in this figure legend, the reader is referred to the web version of this article.)

The inhibitory coupling was organized in the same manner as excitatory one, but with $k<0$. The pulse from the driving neuron comes to the driven one and suppresses its activity. If the driven generator was generating it can stop since its summary potential becomes less than 0, with its pulses no longer spreading across the network. If the driven neuron was not generating, inhibitory pulse leads to additional overinhibition, which will be compensated with time by itself, since the cell tends to keep the constant resting state potential about −70 mV. Normally, the same neurons achieve both excitatory and inhibitory inputs and the resulting activity depends on their amount and synchrony.

In the mathematical model the driving signal was put into the activation function (2) with $k = \pm 1$, providing excitatory and inhibitory couplings respectively. In the circuit inhibitory and excitatory couplings were organized by a switch. To test the electrical synapse (Fig. 2) for

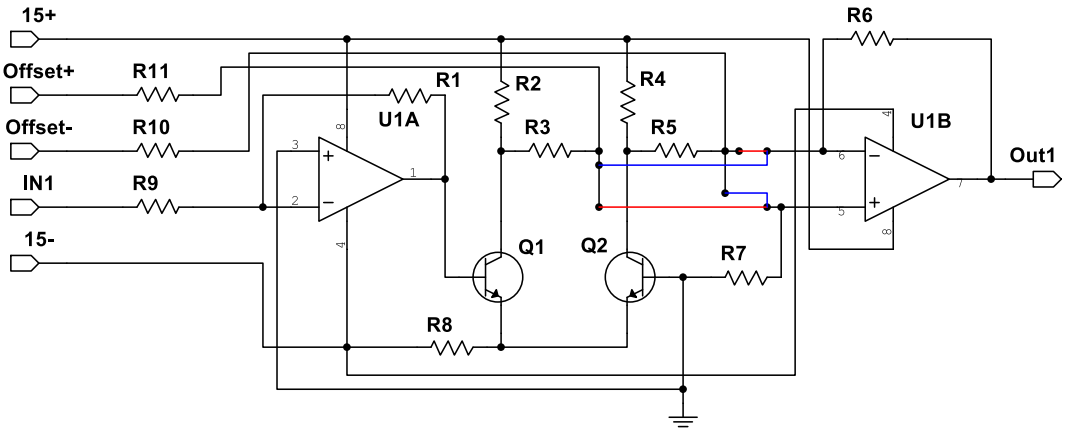

Fig. 2. Circuit diagram of the sigmoid activation function in form hyperbolic tangent function. $R1 = 0.51$ kΩ, $R2 = R4 = 1$ kΩ, $R3 = R5 = R9 = R10 = R11 = 10$ kΩ, $R6 = R7 = 5.1$ kΩ, $R8 = 2$ kΩ, Q1, Q2 are bipolar junction transistors 2 N1711, U1 is an amplifier of the type NE5532AI. Red color is for excitatory coupling, blue color is for inhibitory coupling. (For interpretation of the references to color in this figure legend, the reader is referred to the web version of this article.)

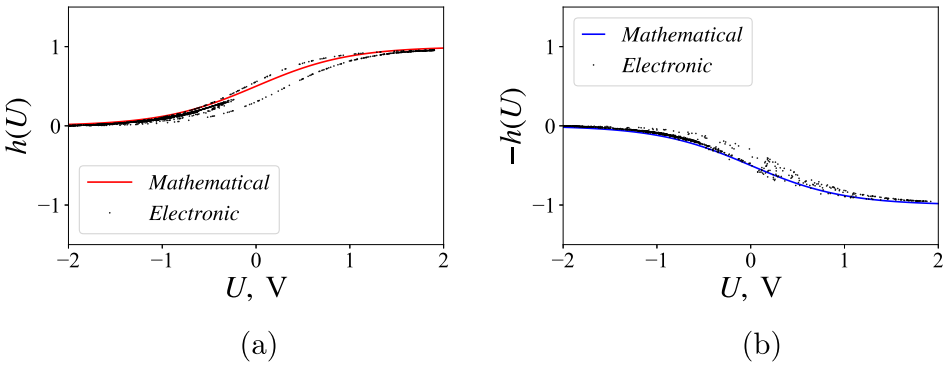

Fig. 3. Experimentally measured nonlinear function (the harmonic driving of 2 V amplitude was applied and response was measured) for excitatory synapse $h(U)$ (a) and for inhibitory synapse $-h(U)$ (b). X-axis: presynaptic signal; Y-axis: postsynaptic signal.

correctness of work, a harmonic signal of 2 V amplitude was introduced as a driving. The resulting nonlinear function was compared to the mathematical model, see Fig. 3). One can see that the simulation of the electronic circuit mostly matches the results of mathematical modeling, but the circuit has a shift in the argument of sigmoid, providing partly different nonlinearity for positive and negative $\frac{dU}{dt}$ (two branches are well established).

5. Two coupled neurons

5.1. Mathematical model

Two neurons were coupled by sigmoid coupling in the mathematical model. Three connectivity mechanisms were considered: unidirectional coupling, bidirectional symmetric coupling (both either excitatory or inhibitory) and bidirectional asymmetric coupling when one neuron excited the other, and the other inhibited the first one. Using Poincare section by the line $u = 0$ in both subsystems, the charts of dynamical regimes were constructed for both oscillators in all considered cases in the same parameter region and with the same step using the series of the same length as previously for a single oscillator. The parameter $k = 1.0$. The parameters a, b were changed synchronously, assuming that in a real networks nearby cells cannot be upset by the parameters significantly.

In the Fig. 4 charts of dynamical regimes for two coupled mathematical neurons at the parameter plane (a, b) were plotted. The blue color corresponds to underfreshold regime (fixed point) in which there is no oscillations. Dark blue area indicates a repeller (no attractor, global instability) regimes. Cyan (light blue) areas correspond to a simple regimes of cycle one. Note, that here and further we consider as regime 1 all types of oscillations for which there is an only positive maximum at a period, since maxima lying in negative subspace (v<0) do not have physiological sense and are considered as under threshold oscillations rather than normal neuron spikes. Green areas correspond to regimes of period 2, i. e. two maxima on the period, including bursts consisting of two spikes or oscillations with spikes of two different amplitudes. Other colors indicate regimes with more complex dynamics. Note, that regime identification was performed using Poincare's section by value $v = 0$ for two neurons (subsystems) separately, so the regime 1 in one neuron can correspond to a regime 2 in another. Further we were especially interested in parameter regions where complex nonlinear oscillations (spikes and bursts) of large amplitude appear from stable point or in addition to it.

When studying unidirectionally coupled neurons, see Fig. 4 (a, b), there is no direct transition from stable point area to areas of complex oscillations (period 2 or higher). All complex regimes are located close to repeller regime, i. e. like in most known classical systems they appear due to simple oscillatory regimes lose their stability.

The analysis of the plots indicates that for the symmetric excitatory coupling (Fig. 4 (c)) new complex regimes appear near the border between the simple limit cycle and attractorless area, though for the symmetric inhibitory coupling (well visible only in Fig. 4 (d) for larger coupling strength) the complex regimes appear between the region of the simple cycle and fixed point area.

The asymmetric coupling provides richer regime set and in larger area than both types of the unidirectional or symmetric one, see Fig. 5. Two interesting zones can be highlighted: Area 1 (a green area separating blue and light-blue areas on Fig. 5 (a)) and Area 2 (a green area on Fig. 5 (c)).

Near the Area 1 transition from excitable nonoscillatory regime to (Fig. 5 (b) the first time series from the top) in a simple oscillatory regime (Fig. 5 (b) the third time series from the top) is carried out through a number of more complex oscillatory regimes of different shape and

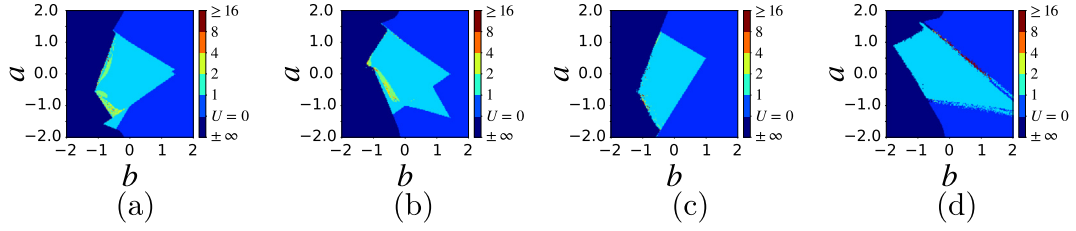

Fig. 4. Charts of dynamical regimes for two coupled mathematical neurons at the parameter plane (a, b). Parameters $\varepsilon = 0.1, c = 1/3, k = 1.0$. Dark blue corresponds to repeller (there is no attractor in the system), blue corresponds to a stable fixed point, cyan corresponds to period one oscillations (one spike per period), green, yellow, orange and red correspond to complex regular oscillatory regimes with different number of spikes per period, burgundy corresponds to chaotic spiking. The subplots are as follows: (a) unidirectional excitatory coupling; (b) unidirectional inhibitory coupling; (c) symmetric excitatory coupling; (d) symmetric inhibitory coupling. (For interpretation of the references to color in this figure legend, the reader is referred to the web version of this article.)

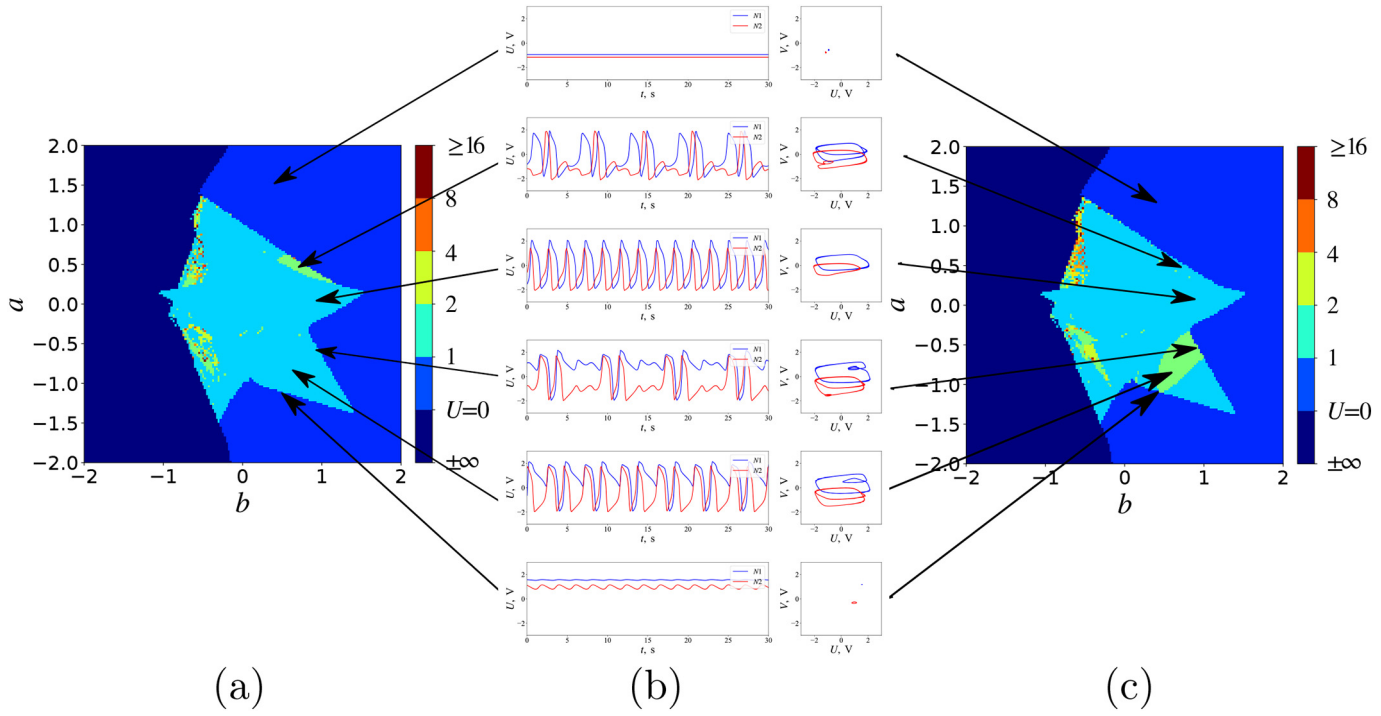

Fig. 5. Charts of dynamical regimes for two bidirectional asymmetric coupled mathematical neurons at the parameter plane (a, b): (a) asymmetric coupling (excitatory driven neuron N1), (c) asymmetric coupling (inhibitory driven neuron N2) and (b) time series in typical regimes (from top to bottom): first $a = 0.292$, $b = 1.126$, second $a = 0.292$, $b = 1.021$, third $a = 0.292$, $b = 1.011$, fourth $a = -0.329$, $b = 0.843$, fifth $a = -0.329$, $b = 0.833$, sixth $a = -1.086$, $b = 0.389$. Parameters $\varepsilon = 0.1$, $c = 1/3$, $k = 1.0$. On the subplots (a,c) colors are as follows: dark blue corresponds to repeller (there is no attractor in the system), blue corresponds to a stable fixed point, cyan corresponds to period one oscillations (one spike per period), green, yellow, orange and red correspond to complex regular oscillatory regimes with different number of spikes per period, burgundy corresponds to chaotic spiking. (For interpretation of the references to color in this figure legend, the reader is referred to the web version of this article.)

period (Fig. 5 (b) the second time series from the top). These complex regimes appear due to a some complex and special nonlocal (global) bifurcation (possibly, saddle-node bifurcation of two cycles). It should be noted that a complex cycle appear directly after the transition from simple regime with a single stable point to bistable regime with both stable point and limit cycle, and then it evaluates to a simple cycle.

In contrary, cycle birth from fixed point in the Area 2 takes place by a classical Andronov–Hopf scenario (Fig. 5 (b), the bottom time series), except possibly the single codimension two point in which green area matches blue one. The Area 2 by itself is a curved triangle, two sides of which are period double bifurcations (between cyan and green areas at Fig. 5 (b)) and the third (the smallest one) side is a saddle-node bifurcation of two (stable and unstable) multibypass limit cycles. These complex cycles consist of a large number of underthreshold oscillations together with two large spikes per period, see Fig. 5 (b) the fourth time series from the top, which evaluate to a more usual period two regime (Fig. 5 (b), the fifth time series from the top) when retreating from the border of oscillation birth/death.

5.2. Electronic realization

The physical representation of two coupled neurons is shown on Fig. 6. Two electronic neurons were coupled by asymmetric sigmoid electronic synapse to detect regimes found in the mathematical model. All regimes shown on Fig. 5 (b) were successfully detected in the circuit too. In addition to these regimes some specific long transient processes like plotted on Fig. 7 were found. This regime was found for $a = 0.487$, $b = 0.88$ (near the border of Area 1). The oscillations were mostly absent first, when they started to rise linearly, then evaluating to high amplitude irregular bursts. The similar oscillations can be found for the mathematical model in Fig. 5 (b), the second time series from the top. Then, these bursts evaluated to simple nonlinear oscillations, see Fig. 5 (b) the third time series from the top. Emergence of such regimes is due to nonstationarity of the circuit, when its actual parameters change with time due to temperature and other physical conditions. Together with nonequality of neurons and synapses and nonideality of their functions as it was shown in Fig. 3, it provides some additional possibilities for realizing complex behavior matching what we see in biological experiment [29].

6. Conclusion and discussion

When constructing electronic circuits of neurons, the synapse construction is of significant significance. There is a number of works

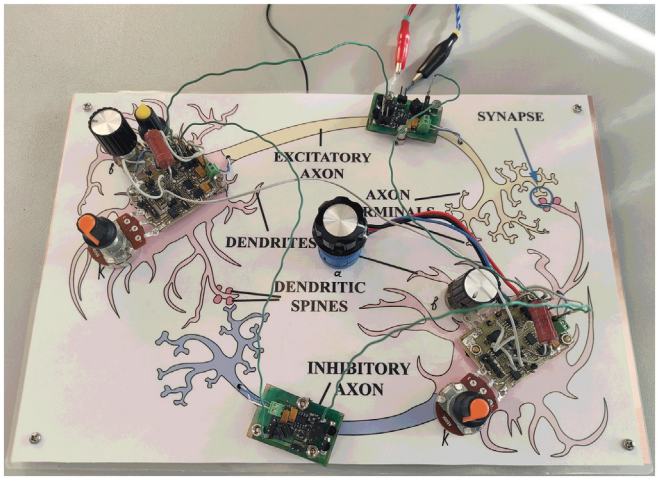

Fig. 6. The photo of the physical representation of the built electric circuit.

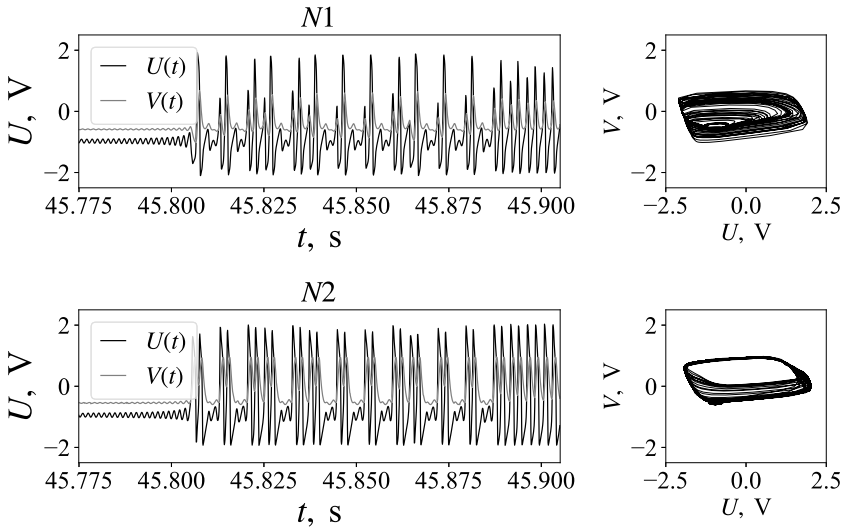

Fig. 7. Time series with transients for electronic realization.

where large ensembles of neurons together with synapses are constructed from semiconductors as a single array [30,31]. Such an approach allows to construct a lot of artificial neurons as a single device, but does not provide any control of the characteristics of individual neurons and synapses, which can vary a lot. Another approach is to construct neuron models and synapses from electronic components like in [7,9]. In contrary, it provides elements with much more predictable properties, so regimes and bifurcations found in mathematical models can be detected in the hardware too. Though large networks are hardly to be implemented following this approach, the direct control of parameters of each element and knowledge of bifurcation mechanisms allow to use such neurons and synapses for modeling real brain phenomena like epilepsy [12].

Here we improved the hardware neuron model developed in [9] by providing realization for nonzero values of the parameter b (see Eq. 1) and developed a new hardware realization of a sigmoid synaptic function, see Eq. 2. We investigated numerically the mathematical model. Two coupled FitzHugh–Nagumo neurons were studied multiply in literature, though in most cases the synchronization between oscillating neurons was considered with nonsigmoid coupling [32,33]. Therefore, we focused on the regimes of activity emerging due to sigmoid coupling in excitable neurons. So, unidirectional connectivity was not studied since for neurons in excitable mode this means no oscillations.

We expect that the main application of the proposed electronic neural model would be generation of some particular types of brain activity. So, among many usual regimes we detected the regimes and bifurcations interesting for further modeling of brain activity. In particular, the idea of use of transient processes instead of stable attractors for modeling the brain functioning was proposed [25] which was supported by particular results in epilepsy modeling [17,26]. Note that both regular and irregular long transient behavior was already found in numerical models of neural networks [34–36], but these results were obtained mostly casually. In our study, in two coupled neurons we found long transient processes and regimes emerging due to nonstationarity of the electronic components. If such regimes can appear near a bifurcation line in a considered simple scheme of two neurons, they (or some similar ones) are very likely to appear in much more complex networks, and therefore, can be considered as valid models of brain dynamics for some normal regimes like sleep and passive wakefulness in which generalized synchronization of large areas is not established and oscillation activity patterns often replace each other [37,38].

CRediT authorship contribution statement

Nikita Egorov: Investigation, Methodology, Visualization, Resources, Software; Ilya Sysoev: Writing - Original draft, Writing - Reviewing and Editing, Formal analysis; Valdimir Ponomarenko: Methodology, Validation, Formal analysis; Marina Sysoeva: Conceptualization, Software, Writing - Original draft, Data Curation, Visualization, Resources, Supervision, Project administration, Funding acquisition.

Declaration of competing interest

Marina V. Sysoeva reports financial support was provided by Russian Science Foundation. Marina V. Sysoeva, Nikita M. Egorov reports a relationship with Yuri Gagarin State Technical University of Saratov that includes: employment.

Acknowledgments

This work was supported by Russian Science Foundation, grant No. 21-72-00015.

References

[1] Mahowald M, Douglast R. A silicon neuron. Nature. 1991;354:515–8.
[2] Hodgkin AL, Huxley AF. A quantitative description of membrane current and its application to conduction and excitation in nerve. J Physiol. 1952;117(4):500–44. https://doi.org/10.1113/jphysiol.1952.sp004764.
[3] Rasche C, Douglas R. An improved silicon neuron. Analog Integr Circuits Signal Process. 2000;23:227–36. https://doi.org/10.1023/A:1008357931826.
[4] van Schaik A. Building blocks for electronic spiking neural networks. Neural Netw. 2001;14(6):617–28. https://doi.org/10.1016/S0893-6080(01)00067-3.
[5] FitzHugh R. Impulses and physiological states in theoretical models of nerve membrane. Biophys J. 1961;1:445–66. https://doi.org/10.1016/S0006-3495(61)86902-6.
[6] Nagumo J, Arimoto S, Yoshizawa S. An active pulse transmission line simulating nerve axon. ProcIRE. 1962;50:2061–70. https://doi.org/10.1109/JRPROC.1962.288235.
[7] Binczak S, Jacquir S, Bilbault J-M, Kazantsev VB, Nekorkin VI. Experimental study of electrical FitzHugh–Nagumo neurons with modified excitability. Neural Netw. 2006;19(5):684–93. https://doi.org/10.1016/j.neunet.2005.07.011.
[8] Li F, Liu Q, Guo H, Zhao Y, Tang J, Ma J. Simulating the electric activity of Fitzhugh-Nagumo neuron by using Josephson junction model. Nonlinear Dyn. 2012;69(4):2169–79. https://doi.org/10.1007/s11071-012-0417-z.
[9] Kulminskiy D, Ponomarenko V, Prokhorov M, Hramov A. Synchronization in ensembles of delay-coupled nonidentical neuronlike oscillators. Nonlinear Dyn. 2019;98(1):735–48. https://doi.org/10.1007/s11071-019-05224-x.
[10] Wang Y, Liu S-C. A two-dimensional configurable active silicon dendritic neuron array. IEEE TransCircSystI: RegPap. 2011;58(9):2159–71. https://doi.org/10.1109/TCSI.2011.2112570.

[11] Ramakrishnan S, Wunderlich R, Hasler J, George S. Neuron array with plastic synapses and programmable dendrites. IEEE Trans Biomed Circuits Syst. 2013;7(5):631–42. https://doi.org/10.1109/TBCAS.2013.2282616.
[12] Egorov NM, Ponomarenko VI, Sysoev IV, Sysoeva MV. Simulation of epileptiform activity using network of neuron-like radio technical oscillators. Technical Phys. 2021;66(3):505–14. https://doi.org/10.21883/JTF.2021.03.50532.237-20.
[13] Egorov NM, Kulminskiy DD, Ponomarenko VI, Sysoev IV, Sysoeva MV. Transient dynamics in electronic neuron-like circuits in application to modeling epileptic seizures. Nonlinear Dyn. 2022. https://doi.org/10.1007/s11071-022-07379-6. in press.
[14] Egorov NM, Ponomarenko VI, Melnikova SN, Sysoev IV, Sysoeva MV. Common mechanisms of attractorless oscillatory regimes in radioengineering models of brain thalamocortical network,Izvestiya VUZ. Appl Nonlinear Dyn. 2021;29(6):927–42. https://doi.org/10.18500/0869-6632-2021-29-6-927-942.
[15] Abbasova KR, Chepurnov SA, Chepurnova NE, van Luijtelaar G. The role of perioral afferentation in the occurrenceof spike-wave discharges in the wag/rij modelof absence epilepsy. Brain Res. 2010;1366:257–62. https://doi.org/10.1016/j.brainres.2010.10.007.
[16] Kapustnikov AA, Sysoeva MV, Sysoev IV. Modeling spike-wave discharges in the brain with small neurooscillator networks. Math Biol Bioinform. 2020;16:139–46. https://doi.org/10.17537/2020.15.138.
[17] Medvedeva TM, Sysoeva MV, Lüttjohann A, van Luijtelaar G, Sysoev IV. Dynamical mesoscale model of absence seizures in genetic models. PLoS ONE. 2020;15(9):e239125. https://doi.org/10.1371/journal.pone.0239125.
[18] Dahlem MA, Hiller G, Panchuk A, Schöll E. Dynamics of delay-coupled excitable neural systems. International Journal of Bifurcation and ChaosNo. 2, 19. Thi is a JOURNAL, not book; 2009; 745–53.
[19] Kopell N, Ermentrout GB, Whittington MA, Traub RD. Gamma rhythms and beta rhythms have different synchronization properties. Proc Natl Acad Sci U S A. 2000;97(4):1867–72. https://doi.org/10.1073/pnas.97.4.1867.
[20] Marreiros AC, Daunizeau J, Kiebel SJ, Friston KJ. Population dynamics: variance and the sigmoid activation function. Neuroimage. 2008;42(1):147–57. https://doi.org/10.1016/j.neuroimage.2008.04.239.
[21] Rabinovich MI, Trubetskov DI. Oscillations and waves in linear and nonlinear systems. Dordrecht: Kluwer Academic Publisher; 1989.https://doi.org/10.1007/978-94-009-1033-1.
[22] Gonchenko SV, Gonchenko AS, Kazakov AO, Kozlov AD, Bakhanova YV. Mathematical theory of dynamical chaos and its applications: review, part 2. Spiral chaos of three-dimensional flows, Izvestiya VUZ. Appl Nonlinear Dyn. 2019;27(5):7–52. https://doi.org/10.18500/0869-6632-2019-27-5-7-52.
[23] Afraimovich VS, Rabinovich MI, Varona P. Heteroclinic contours in neural ensembles and the winnerless competition principle. Int J Bifurcat Chaos. 2004;14(04):1195–208. https://doi.org/10.1142/S0218127404009806.
[24] Afraimovich V, Tristan I, Varona P, Rabinovich M. Transient dynamics in complex systems: heteroclinic sequences with multidimensional unstable manifolds. Discontin Nonlinear Complex. 2013;2(1):21–41. https://doi.org/10.5890/DNC.2012.11.001.
[25] Rabinovich MI, Zaks MA, Varona P. Sequential dynamics of complex networks in mind: consciousness and creativity. Phys Rep. 2020;883:1–32. https://doi.org/10.1016/j.physrep.2020.08.003.
[26] Kapustnikov AA, Sysoeva MV, Sysoev IV. Transient dynamics in a class of mathematical models of epileptic seizures. Commun Nonlinear Sci Numer Simul. 2022;109:106284. https://doi.org/10.1016/j.cnsns.2022.106284.
[27] Richards FJ. A flexible growth function for empirical use. J Exp Bot. 1959;10(2):290–300. https://doi.org/10.1093/jxb/10.2.290.
[28] Li H, Yang Y, Li W, He S, Li C. Extremely rich dynamics in a memristor-based chaotic system. Eur Phys J Plus. 2020;135:579. https://doi.org/10.1140/epjp/s13360-020-00569-4.
[29] Wu SH, Kelly JB. Physiological properties of neurons in the mouse superior olive: membrane characteristics and postsynaptic responses studied in vitro. J Neurophysiol. 1991;65(2):230–46. https://doi.org/10.1152/jn.1991.65.2.230.
[30] Jackson BL, Rajendran B, Corrado GS, Breitwisch M, Burr GW, Cheek R, et al. Nanoscale electronic synapses using phase change devices. J Emerg Technol Comput Syst. 2013;9(2). https://doi.org/10.1145/2463585.2463588.
[31] Eryilmaz SB, Neftci E, Joshi S, Kim S, BrightSky M, Lung H-L, et al. Training a probabilistic graphical model with resistive switching electronic synapses. IEEE Trans Electron Devices. 2016;63(12):5004–11. https://doi.org/10.1109/TED.2016.2616483.
[32] Hoff A, Dos Santos JV, Manchein C, Albuquerque HA. Numerical bifurcation analysis of two coupled Fitzhugh-Nagumo oscillators. Eur Phys J B. 2014;87(7):151. https://doi.org/10.1140/epjb/e2014-50170-9.
[33] Plotnikov SA, Fradkov AL. On synchronization in heterogeneous Fitzhugh–Nagumo networks. Chaos, Solitons & Fractals. 2019;121:85–91. https://doi.org/10.1016/j.chaos.2019.02.006.
[34] van Ooytien A, van Pelt J, Corner MA, Lopes da Silva FH. The emergence of long-lasting transients of activity in simple neural networks. Biol Cybernetics. 1992;67:269–77. https://doi.org/10.1007/BF00204400.
[35] Riecke H, Roxin A, Madruga S, Solla SA. Multiple attractors, long chaotic transients, and failure in small-world networks of excitable neurons. Chaos. 2007;17(2):026110. https://doi.org/10.1063/1.2743611.
[36] Sysoev IV, Ponomarenko VI, Prokhorov MD. Reconstruction of ensembles of nonlinear neurooscillators with sigmoid coupling function. Nonlinear Dyn. 2019;95(3):2103–16. https://doi.org/10.1007/s11071-018-4679-y.
[37] Buzsáki G. Rhythms of the brain. Oxford University Press; 2006.
[38] Watson BO, Buzsáki G. Sleep, memory and brain rhythms. Daedalus. 2015;144(1):67–82. https://doi.org/10.1162/DAED_a_00318.